



Published in final edited form as:

*Oncogene*. 2020 May ; 39(19): 3910–3925. doi:10.1038/s41388-020-1261-0.

## Tetraspanin CD82 drives Acute Myeloid Leukemia chemoresistance by modulating Protein Kinase C alpha and $\beta 1$ integrin activation

Muskan Floren<sup>1</sup>, Sebastian Restrepo Cruz<sup>1</sup>, Christina M. Termini<sup>1</sup>, Kristopher D. Marjon<sup>1</sup>, Keith A. Lidke<sup>2,3</sup>, Jennifer M. Gillette<sup>1,3,\*</sup>

<sup>1</sup>Department of Pathology, University of New Mexico Health Sciences Center, Albuquerque, NM 87131

<sup>2</sup>Department of Physics and Astronomy, University of New Mexico, Albuquerque, NM 87131

<sup>3</sup>UNM Comprehensive Cancer Center, Albuquerque, NM 87131

### Abstract

A principal challenge in treating acute myeloid leukemia (AML) is chemotherapy refractory disease. As such, there remains a critical need to identify key regulators of chemotherapy resistance in AML. In this study, we demonstrate that the membrane scaffold, CD82, contributes to the chemoresistant phenotype of AML. Using an RNA-seq approach, we identified the increased expression of the tetraspanin family member, CD82, in response to the chemotherapeutic, daunorubicin. Analysis of the TARGET and BEAT AML databases identifies a correlation between CD82 expression and overall survival of AML patients. Moreover, using a combination of cell lines and patient samples, we find that CD82 overexpression results in significantly reduced cell death in response to chemotherapy. Investigation of the mechanism by which CD82 promotes AML survival in response to chemotherapy identified a crucial role for enhanced protein kinase c alpha (PKC $\alpha$ ) signaling and downstream activation of the  $\beta 1$  integrin. Additionally, analysis of  $\beta 1$  integrin clustering by super-resolution imaging demonstrates that CD82 expression promotes the formation of dense  $\beta 1$  integrin membrane clusters. Lastly, evaluation of survival signaling following daunorubicin treatment identified robust activation of p38 mitogen-activated protein kinase (MAPK) downstream of PKC $\alpha$  and  $\beta 1$  integrin signaling when CD82 is overexpressed. Together, these data propose a mechanism where CD82 promotes chemoresistance by increasing PKC $\alpha$  activation and downstream activation/clustering of  $\beta 1$  integrin, leading to AML cell survival via activation of p38 MAPK. These observations suggest that the CD82-PKC $\alpha$  signaling axis may be a potential therapeutic target for attenuating chemoresistance signaling in AML.

---

Users may view, print, copy, and download text and data-mine the content in such documents, for the purposes of academic research, subject always to the full Conditions of use:[http://www.nature.com/authors/editorial\\_policies/license.html#terms](http://www.nature.com/authors/editorial_policies/license.html#terms)

\*corresponding author: [jgillette@salud.unm.edu](mailto:jgillette@salud.unm.edu).

Competing Interests

All authors declare no competing financial interests in relation to the work described.

## Introduction

Acute myeloid leukemia (AML) is characterized by the disruption of myeloid differentiation and accumulation of blast cells in the bone marrow. In 2019, AML is estimated to be the most prevalent newly diagnosed leukemia and the leading cause of leukemia-related mortality (1). Response to therapy differs widely between AML subclasses due to the highly heterogeneous characteristics of the disease at both the phenotypic and molecular level. The standard induction therapy for AML: cytarabine for seven consecutive days and daunorubicin on the first three days, is effective in a small subset of AML patients, but most patients are not cured and long-term disease-free survival remains poor (2). With a chemotherapy-only treatment regimen, less than 40% of adult patients achieve disease-free survival greater than 5 years; the disease free-survival rate is further reduced in younger patients (3). Chemoresistance is largely responsible for treatment failure and overall reduced survival in AML. Therefore, there is a critical need to identify key regulators of chemotherapy resistance in AML.

While specific mechanisms of drug resistance in AML remain poorly defined, many studies suggest that resistance may be a result of multiple factors. Some of the most recognized mechanisms of drug resistance in AML include genetic alterations, drug resistance-related proteins, miRNAs alterations, and aberrant activation of drug resistance-related signaling pathways (4, 5). For example, Fms-like tyrosine kinase 3 (FLT3) mutations found in one-third of patients with AML constitutively activates the kinase resulting in aberrant proliferation, which supports AML cell survival upon treatment with conventional chemotherapeutics (6, 7). The activation of additional signaling pathways including PI3K/AKT, JAK/STAT and NF- $\kappa$ B have also been reported as survival mechanisms for drug resistance in AML (8–11).

Tetraspanins, a family of membrane scaffolding proteins, function as regulators of cellular signaling through the organization of membrane microdomains consisting of membrane receptors and effector signaling molecules (12). Tetraspanins were shown to be involved in tumor progression at many stages including: angiogenesis, metastasis, and therapy resistance (13). With respect to AML, Tetraspanin 3 was recently demonstrated to play a role in the development of de novo AML (14), whereas tetraspanin CD81 was identified as an unfavorable prognostic marker in AML (15).

The tetraspanin CD82 was also found to be upregulated in several leukemias, including AML (16), with aberrant CD82 expression detected specifically in chemotherapy-resistant CD34<sup>+</sup>/CD38<sup>-</sup> AML cells (17, 18). Additionally, work from our group identified CD82 as a key regulator of AML cell homing to the bone marrow (19) and demonstrated that CD82 modulates the spatial and temporal dynamics of Protein Kinase C  $\alpha$  (PKC $\alpha$ ) signaling in AML (20). Interestingly, PKC $\alpha$  expression was shown to correlate with poor survival in AML patients and contribute to cancer progression (21). Moreover, targeting PKC-mediated signaling stimulated an increase in apoptosis of AML cells (22). In the present study, we identify CD82 as a tetraspanin upregulated in response to chemotherapy in AML. Moreover, we demonstrate that tetraspanin CD82 promotes chemoresistance in AML cells and delineate a mechanism involving integrin  $\beta$ 1 and p38 MAPK activation downstream of

PKC $\alpha$  signaling, providing valuable targets for further development of therapies to treat chemotherapy-resistant AML.

## Results

### Chemotherapy increases the expression of tetraspanins CD82 and CD53 in AML.

To evaluate how tetraspanin expression is modulated by AML cells in response to chemotherapy, we completed a RNA-sequencing (RNA-seq) study using the AML cell line (KG1a) treated with the conventional chemotherapeutic, daunorubicin. Analysis of tetraspanin family members identified transcriptional alterations following chemotherapy (Fig. 1A). Most notably, daunorubicin treatment stimulated the expression of tetraspanins CD82 and CD53 (Fig. 1A). Next, we subjected multiple AML cell lines (KG1a, Kasumi-1 and HL-60) representing the most prevalent and undifferentiated stem-like M1 and M2 subtypes (Fig. 1B, Supp. Table 1), to treatment with daunorubicin and measured the surface expression changes of both CD82 and CD53 (23–26). Flow cytometry analysis established that CD82 expression is significantly increased on the surface of all cell lines analyzed in response to chemotherapy (Fig. 1C,D). In contrast, CD53 expression is increased in the KG1a cells only, with no differences detected in the Kasumi-1 or HL-60 cells (Fig. 1E,F). Lastly, two AML patient samples were analyzed for CD82 expression before and after daunorubicin treatment, again identifying a significant upregulation of surface CD82 expression following chemotherapy (Fig. 1G). Collectively, these data suggest that the tetraspanin CD82 is upregulated in response to chemotherapy and thus may stimulate a critical survival signaling cascade.

### Increased CD82 expression in AML patient samples correlates with reduced overall survival.

To determine whether CD82 overexpression could be an indicator of patient outcomes, we analyzed the Therapeutically Applicable Research to Generate Effective Treatment (TARGET) AML database, which included RNA-seq analysis of 152 primary AML patient samples, of which 125 samples were collected from bone marrow aspirates and categorized into even-sized groups based on tertiles. Examination of survival outcomes based on CD82 (Fig. 2A) or CD53 (Fig. 2B) expression identifies poor overall survival in patients aged 0-24 with increased CD82 expression, but not CD53. To investigate how CD82 expression impacts adult AML patient outcomes, we analyzed overall survival data from the BEAT AML trial (310 patients, ages 25-74). Patients were further classified into two age groups of 25-49 (n=86) and 50-74 (n=224). Increased CD82 expression predicted an increased hazard ratio (HR) of 1.4 (CI: 0.72-2.89) for overall survival ages 25-49 (Fig. 2C) and a smaller ratio of 1.1 (CI: 0.76-1.52) in the 50-74 group (Fig. 2E). In contrast, comparison of survival outcomes between CD53 high to low expression predicted a HR of 1.2 (CI: 0.68-2.50) for ages 25-49 (Fig. 2D) and 1.0 (CI: 0.76-1.48) for ages 50-74 (Fig. 2F). In combination, our analyses indicate a correlation between increased CD82 expression and reduced overall survival in both pediatric and adult AML patients, further implicating a role for CD82 in AML survival.

### **CD82 overexpression promotes AML chemoresistance.**

Recognizing the critical role of chemoresistance in overall AML survival and relapse, we went on to determine the impact of CD82 expression on AML cell response to chemotherapy *in vitro*. AML cell lines (KG1a and Kasumi-1) were generated with CD82 overexpression (CD82OE), CD82 knock down (CD82KD), and vector control cells (control). Cells were treated with standard induction therapy agents daunorubicin (1.7 $\mu$ M) or cytarabine (0.5 $\mu$ M) for 72 hours. Caspase 3/7 activation analysis by flow cytometry indicates that CD82OE cells display reduced apoptosis in response to chemotherapy when compared to control cells (Fig. 3A–D). Moreover, CD82KD cells display enhanced cell death following chemotherapy treatment, further implicating an important role for CD82 expression in AML response to chemotherapy (Fig. 3A–C). CD82OE cells also show a decrease in apoptosis as detected by confocal imaging of annexin V positive cells (green) following daunorubicin treatment (Fig. 3E). Taken together, these data support the findings that CD82 expression modulates chemotherapy-mediated apoptosis in AML cells.

### **PKC $\alpha$ is required for CD82-mediated chemoresistance.**

To investigate the mechanism by which CD82 promotes AML chemoresistance and cell survival, we completed RNA-seq experiments with the CD82OE cells treated with and without daunorubicin. When compared to control cells, the combination of daunorubicin treatment and CD82 overexpression led to significant transcriptomic alterations, with over 6000 genes differentially expressed with both P-value and false discovery rate (FDR) <0.05. Principal component analysis displays differential clustering between control and CD82OE cells following vehicle or daunorubicin treatment (Fig. 4A). Of particular interest, *PRKCA* gene expression was increased upon CD82 overexpression and further increased following daunorubicin treatment as indicated on the heat map (Fig. 4A). Our previous work identified a critical role for CD82 in the regulation of PKC $\alpha$  activation (20), thus we went on to measure potential changes in PKC $\alpha$  expression and activation in response to chemotherapy treatment. Western blot analysis indicates that CD82 overexpression significantly increases phospho-PKC $\alpha$  expression following daunorubicin treatment (Fig. 4B–E). To determine whether the expression and/or activation of PKC $\alpha$  contributes to the chemoresistant phenotype of CD82OE cells, we utilized both pharmacologic (Fig. 4F) and genetic inhibition (Fig. 4G,H) of PKC $\alpha$  and evaluated cell death response to daunorubicin. Caspase activity assays demonstrate that while PKC $\alpha$  inhibition has no effect on cell death of control cells or CD82KD cells (Supp. Fig 1), PKC $\alpha$  inhibition in combination with daunorubicin increases cell death of CD82OE cells, restoring chemosensitivity to that of control cells. Therefore, PKC $\alpha$  is a critical signaling component of CD82-mediated chemoresistance in AML.

### **Chemotherapy activates $\beta$ 1 integrin downstream of PKC $\alpha$ .**

PKC $\alpha$  regulates a number of key biological events including proliferation and differentiation (27–30). Moreover, PKC $\alpha$  interacts with a number of downstream targets that support cell survival. Further analysis of the transcriptional patterns of CD82OE cells following daunorubicin treatment identified enrichment of the MAPK signaling for integrins biological pathway (Fig. 5A). This transcriptional signature led us to investigate the impact of CD82

expression on the integrin signaling activity of daunorubicin-treated AML cell lines. Flow cytometry analyses of total surface  $\beta 1$  integrin show minimal expression changes between control or CD82OE cells with or without daunorubicin treatment (Fig. 5B). In contrast, CD82 overexpression and daunorubicin treatment both increase the activation of  $\beta 1$  integrin in the KG1a and Kasumi-1 cells with the greatest increase in  $\beta 1$  activity detected in the CD82OE cells treated with daunorubicin (Fig. 5C–E). We also analyzed the  $\beta 1$  activity of AML patient samples following daunorubicin treatment, identifying a 1.4-fold and 1.8-fold increase in  $\beta 1$  activity in patients 39 and 75, respectively (Fig. 5F). Taken together, daunorubicin treatment and CD82 overexpression both stimulate the activation of  $\beta 1$  integrin. Recognizing the critical role PKC $\alpha$  activity plays in both upstream (inside-out) and downstream (outside-in) integrin signaling, we repeated the  $\beta 1$  activity assay in the presence of PKC $\alpha$  inhibition. Both pharmacologic (Fig. 5C) and genetic (Fig. 5D) inhibition of PKC $\alpha$  attenuated the  $\beta 1$  activation observed upon CD82 overexpression and daunorubicin treatment, suggesting that PKC $\alpha$  signaling is upstream of chemotherapy-induced  $\beta 1$  activation. PKC $\alpha$  promotes talin-1 activation and binding to the  $\beta 1$  integrin tail, which is a critical final step in inside-out integrin activation stimulating  $\beta 1$  activation (31). Next, we quantified talin-1 phosphorylation, finding a significant increase in talin-1 activation in CD82OE cells that is further increased upon daunorubicin treatment (Fig. 5G). Lastly, to confirm that  $\beta 1$  activation is a critical player in CD82-mediated chemoresistance, we incorporated BIO 5192, a previously characterized selective small molecule inhibitor of both the activated and inactivated forms of  $\alpha 4\beta 1$  integrin (32). Figure 5H displays increased cell death in the BIO 5192-treated CD82OE cells upon daunorubicin treatment, consistent with a recovery of chemosensitivity. Collectively, these data suggest that PKC $\alpha$ -stimulated inside-out signaling of the  $\beta 1$  integrin is the primary signaling pathway responsible for CD82-mediated AML chemoresistance.

### **CD82 expression alters $\beta 1$ integrin membrane clustering.**

Inside-out signaling can also stimulate the clustering of integrins in the membrane, which can modulate integrin avidity, promoting cell adhesion and signaling (33, 34). Therefore, we next used the super-resolution imaging (SRI) technique, direct stochastic optical reconstruction microscopy (dSTORM), to measure changes in  $\beta 1$  integrin membrane organization following CD82 overexpression and/or chemotherapy treatment. Figures 6A,B illustrate representative dSTORM images that were analyzed by the density-based spatial clustering of applications with noise (DBSCAN) algorithm to quantify  $\beta 1$  clustering (35). DBSCAN analysis identified significant changes in the organization of  $\beta 1$  clusters, finding that CD82 overexpression promotes an increased number of smaller-sized clusters when compared to control cells (Fig. 6C,E). Moreover, nearest neighbor analysis suggests that  $\beta 1$  clusters are in closer proximity with each other (Fig. 6D) and more densely packed (Fig. 6F) upon CD82 overexpression. In contrast, daunorubicin treatment appears to have minimal impact on  $\beta 1$  integrin membrane distribution (Fig. 6B–F). Therefore, when taken together, SRI analyses suggest that CD82 overexpression significantly contributes to  $\beta 1$  integrin organization, which can modulate downstream survival signaling.

### **p38 MAPK is activated upon chemotherapy treatment in AML.**

Chemotherapy agents stimulate DNA damage and are also strong activators of the p38 MAPK pathway (36, 37). Activation of p38 can enhance cancer cell survival, with increasing evidence suggesting that p38 $\alpha$  facilitates tumor chemoresistance (38). Integrin signaling is frequently linked to p38 activation (39, 40), thus, we evaluated p38 signaling downstream of PKC $\alpha$  and  $\beta$ 1 integrin. Using western blot analysis, we measured total and phospho-p38 following chemotherapy treatment alone or in combination with PKC $\alpha$  or  $\beta$ 1 integrin inhibition. We find no changes in total p38 expression (Fig. 7A,B), but detect a significant increase in phospho-p38 expression upon chemotherapy treatment in control cells that is enhanced by CD82 overexpression (Fig. 7A,C). Inhibition of PKC $\alpha$  in combination with chemotherapy treatment significantly reduced the activation of p38 detected, supporting a role for p38 activation downstream of PKC $\alpha$  signaling (Fig. 7A,C). Additionally, inhibition of  $\alpha$ 4 $\beta$ 1 combined with chemotherapy also shows a reduction in phospho-p38 when compared to chemotherapy treatment alone (Fig. 7D,F), with no change in total p38 expression (Fig. 7D,E). Lastly, we went on to pharmacologically inhibit p38 activity and analyze response to chemotherapy. While we detect no change in response to chemotherapy in control cells, we measure an overall increase in chemosensitivity in CD82 overexpressing cells upon p38 inhibition (Fig. 7G). Collectively, these data demonstrate that CD82 overexpression promotes chemoresistance in AML cells via p38 activation downstream of PKC $\alpha$  and  $\beta$ 1 integrin mediated signaling (Fig. 7H).

### **Discussion**

A major challenge in treating AML is the development of resistant disease resulting in relapse. Numerous studies have focused on identifying important molecules and pathways associated with chemoresistance mechanisms in aggressive hematologic malignancies with the goal of eliminating disease relapse. Aberrant activation of drug resistance-related signaling proteins represents a critical mechanism in AML chemoresistance currently being explored (5). In this study, we investigate AML cell signaling response to chemotherapeutics with a focus on the tetraspanin family of membrane scaffold proteins.

Tetraspanins are widely and abundantly expressed in multiple malignancies and have been described to promote various cancer stages including initiation (13), progression (14), and metastasis (12, 16, 19). Additionally, evidence suggests supporting roles for tetraspanins in cancer drug resistance. Specifically, CD151 (41), Tspan12 (42), CD9 and CD81 (43, 44) have all been shown to modulate cancer cell response to various chemotherapy agents. Using RNA-seq to pursue an unbiased assessment of potential tetraspanins involved in chemoresistance, we identify the upregulation of two specific tetraspanins, CD53 and CD82. Further analysis of cell lines and patient samples illustrates that CD82 expression is significantly enhanced following chemotherapy across all samples analyzed. Our subsequent analysis of the TARGET and BEAT AML databases identified a significant correlation between CD82 expression and overall AML patient survival. These aggregate findings led us to focus our study on CD82, which has been shown to have key signaling roles in AML (18, 45–48).

CD82 was originally identified as a suppressor of tumor migration, invasion and metastasis in malignancies including prostate, breast and lung (49–51). In hematology, CD82 was identified on early hematopoietic progenitor cells and found to be upregulated in distinct human leukemias including AML (16). CD82 was shown to regulate adhesion, survival and bone marrow homing of AML (52) and identified in a proteomics screen to be enriched in the plasma membrane of leukemia stem cells (48). In the current study, we find that CD82 overexpression in AML reduces apoptosis in response to conventional chemotherapeutics. Furthermore, we find that chemosensitivity is restored following CD82 knock down. Thus, CD82 expression modulates AML response to chemotherapy. Our findings are supported by a recent study investigating pediatric AML, which identified an upregulation of CD82 gene expression in AML cells isolated from the bone marrow and went on to find that increased CD82 expression promoted adriamycin chemoresistance (46). Collectively, these data suggest that CD82 expression has the capacity to regulate AML survival signaling in response to chemotherapy.

Previously, STAT5 (45, 47) and Wnt/ $\beta$ -catenin signaling (46) were described to impact CD82-mediated survival signaling of AML. Our RNA-seq analysis of CD82OE cells identified significant expression changes in 6810 genes, including upregulation of *PKRCA* following daunorubicin treatment. Increased PKC $\alpha$  activation was correlated with poor survival rates in AML patients (21) and increased AML cell viability (27, 53). Work from our lab discovered that the CD82 membrane scaffold stabilizes activated PKC $\alpha$  at the plasma membrane in response to stimulation, resulting in aberrant sustained ERK activation (20). Here, we find that CD82 overexpression contributes to enhanced PKC $\alpha$  activation following chemotherapeutic treatment, and that inhibition of PKC $\alpha$  can restore chemosensitivity of CD82OE cells. These data suggest that PKC $\alpha$  activation is a critical regulator of CD82-mediated chemoresistance. The classical PKC isoforms alpha and beta are known to support survival signaling, and thus have been explored as potential targets for anti-cancer therapies. Enzastaurin, the PKC $\beta$  inhibitor, was shown to stimulate apoptosis in AML-derived cell lines and in blast cells from AML patients at concentrations that also inhibit PKC $\alpha$  (53). Clinical trials involving PKC inhibitors as single therapies have been inconsistent (54–56), however, the results of our study suggest that stratification of patients based on CD82 expression could potentially improve response to PKC specific therapies.

PKC activation functions in both inside-out and outside-in integrin signaling, which can contribute to chemoresistance (57–60). Pathway analysis of the transcriptional signature of CD82OE cells following daunorubicin treatment identified the upregulation of MAPK signaling for integrins. In the presence of environmental and therapeutic stresses, integrins can function in the absence of ligand binding to promote survival and a “stemness” phenotype (61). We find that chemotherapy treatment and CD82 overexpression increase  $\beta$ 1 activation in AML cell lines and patient samples. Interestingly,  $\beta$ 1 activation is reduced back to basal signaling upon PKC $\alpha$  inhibition by pharmacologic or genetic knock-down, suggesting that PKC $\alpha$  is signaling upstream of  $\beta$ 1 integrin activation. Also consistent with inside-out signaling, we detect talin-1 activation in CD82OE treated with daunorubicin. Additionally, the restored chemosensitivity of CD82OE cells following treatment with the  $\alpha$ 4 $\beta$ 1 inhibitor is supported by recent findings in T-Acute Lymphoblastic Leukemia where blockade of  $\beta$ 1 integrin sensitized xenografted leukemic cells to doxorubicin and diminished

leukemic burden in the bone marrow (62). Collectively, our work supports a previously proposed concept where a tetraspanin-PKC-integrin complex is essential for signaling (63) and goes on to suggest that the level of CD82 expression serves as a modulator of signal intensity and perhaps signal duration critical for chemoresistance.

Membrane clustering of integrins is fundamental for integrin signaling where interactions with scaffold proteins, including tetraspanins, have been shown previously to modulate the formation of integrin clusters (64). Using SRI, we identify significant changes in  $\beta 1$  cluster organization and density when CD82 is overexpressed in AML cells. Specifically, we find an increase in  $\beta 1$  integrin packing into smaller scale clusters upon CD82 overexpression, which is likely to contribute to the measured increase in  $\beta 1$  activation. Previous work from our group identified similar density changes with integrin  $\alpha 4$  upon CD82 overexpression, which significantly altered cell adhesion (64) and we went on to show that enhanced membrane clustering of PKC $\alpha$  promoted by CD82 resulted in a sustained signaling response (20). Therefore, when taken together, CD82 not only promotes the stabilized signaling of PKC $\alpha$ , but also enhances the membrane clustering of integrins, which collectively can have significant impacts on downstream survival signaling.

The p38 MAPK pathway is activated in response to a host of cellular stressors. The well-defined role of p38 in cell growth inhibition and apoptosis has led to its characterization as a tumor suppressor protein, but p38 also functions in the less well-characterized function of cell survival (36). In fact, p38 often facilitates tumor cell survival in response to chemotherapeutic treatments (37, 38). Our data demonstrate that following daunorubicin treatment the p38 signaling pathway is activated in AML cells. More importantly, CD82 overexpression leads to a significant increase in p38 activation in response to daunorubicin. Inhibition of PKC $\alpha$  and  $\alpha 4\beta 1$  activation in combination with daunorubicin treatment resulted in attenuated p38 signaling. Moreover, p38 inhibition restored chemosensitivity of CD82 overexpressing cells. Thus, p38 inhibitors, which have been investigated in the treatment of myelodysplastic syndrome and AML (65, 66) may also provide benefit to AML patients with increased CD82 expression.

A better understanding of the cellular mechanisms that can be exploited to restore AML sensitivity to chemotherapy is a critical requirement to improving long-term treatments for patients. In this study we identify the CD82 scaffold as a modulator of survival signaling in response to chemotherapeutic agents, resulting in chemoresistance. Tetraspanins are currently being used in clinical trials for the treatment of other hematological malignancies (67) and our data suggest that targeting the CD82 scaffold may provide a mechanism to disrupt the aberrant signaling that contributes to chemotherapeutic response. Therefore, the ability to disrupt the CD82 membrane scaffold, which we show serves to stimulate PKC $\alpha$ ,  $\beta 1$  integrin and p38 activation (three critical drivers of cell survival signaling) may represent a novel approach to treat chemoresistant AML.



## Materials and Methods

### Cell culture

KG1a, Kasumi-1 and HL-60 cells (American Type Culture Collection) were cultured in RPMI 1640 or IMDM supplemented with 10%FBS, 2 mM l-glutamine, 100 u/ml penicillin, and 100 µg/ml streptomycin. Nucleofections were performed using Amaxa Cell Line Nucleofector Kit V (Lonza) according to the manufacturer's directions. G418 was used to generate stable cell lines. Stable CD82 knockdown was established using KG1a cells transfected with the CD82 shRNA plasmid (Santa Cruz Biotechnology, sc-35734-SH); cells were put under puromycin selection and sorted for negative CD82 surface expression. PKCα shRNA plasmid (Santa Cruz Biotechnology; sc-36243-SH) was used for PKCα knockdown.

### RNA-Sequencing

Total RNA was extracted from KG1a WT and CD82OE cell lines treated with 1.7µM Daunorubicin or vehicle control using the RNeasy Mini Kit (QIAGEN). Synthesis of cDNA and library preparation were performed using the SMARTer Universal Low Input RNA Kit for Sequencing (Clontech) and the Ion Plus Fragment Library Kit (ThermoFisher) as previously described (68–70). Library was quality checked on an Agilent DNA High Sensitivity Chip and quantified using qPCR. Samples are diluted to 50-100 pM and pooled in equalmolar concentrations prior to loading into the Ion Chef for emulsion, enrichment, and chip loading. All libraries were sequenced on 540 chips using the Ion Proton S5/XL systems (Life Technologies) in the Analytical and Translational Genomics Shared Resource at the University of New Mexico Comprehensive Cancer Center. All samples were aligned with Torrent Mapping Alignment Program (TMAP, v5.2.25), to a BED file containing non-overlapping exons from UCSC genome hg19. Exon feature counts were generated with HTSeq-count (71). Normalized data was used for analysis of differentially expressed genes (DEGs) between the *CD82OE* and wild-type cells were identified by using R packages DESeq2 and edgeR (72, 73) using the following criteria:  $|\log_2 \text{fold change (FC)}| \geq 2$ , for both P-value and false discovery rate (FDR)  $< 0.05$ , heatmaps was generated using JavaTreeview and pathway analysis was conducted using Metascape.(74, 75). RNA sequencing data is available for download from the NCBI BioProject database using study accession number PRJNA601161

Patient bone marrow aspirate RNA sequencing data was available through the TARGET website (<https://ocg.cancer.gov/programs/target>) and available under database of Genotypes and Phenotypes (dbGaP) accession number phs000465 (n= 125). Beat AML trial data was available through the (<http://vizome.org/aml/>) (n=310).

### Clinical Samples

AML patient samples were deidentified and obtained from the Human Tissue Repository and Cell Analysis Shared Resource at the University of New Mexico Health Sciences Center. All samples were collected with informed consent of the donors and studies were conducted in accordance with the principles of the Declaration of Helsinki. All studies were performed under Institutional Review Board-approved protocols.

### Caspase-3/-7 activity assay

Cells treatments were as follows: 1.7 $\mu$ M Daunorubicin (chemotherapy, Sigma-Aldrich), 1 $\mu$ M Cytarabine (chemotherapy, Tocris), 1 $\mu$ M GO6976 (PKC inhibitor, Tocris), 20nM BIO5192 (VLA-4 inhibitor, Tocris) or 25nM BMS 582949 (p38 MAP kinase inhibitor, Cayman Chemical) individually or in combination as stated. Caspase-3/-7 activity was measured with the CellEvent™ Caspase-3/7 Green Flow Cytometry Assay Kit as indicated by manufacturer (Thermo Fisher). Cells were analyzed using an Accuri C6 flow cytometer (BD Bioscience) and percent caspase positive cells were normalized to unstained controls.

### Flow Cytometry

Cells were labeled with antibody or the corresponding isotype control in 1% BSA/PBS for 30 mins on ice. Cells were washed and analyzed using an Accuri C6 flow cytometer (BD Bioscience); histograms were generated using FlowJo software. Mean fluorescence values were normalized to the control cell line level. Antibodies used were CD82-Alexa-647 (Biolegend, ASL-24), CD53-PE (BioLegend, HI29), and Integrin  $\beta$ 1-Alexa-647 (BioLegend, TS2/16). For active  $\beta$ 1 integrin expression, cells were labeled with Ligand-induced binding site (LIBS) Anti-Integrin  $\beta$ 1 Antibody (Millipore, HUTS-4) for 30 mins. Cells were washed and labeled with goat anti-mouse Alexa-647 secondary antibody (Invitrogen).

### Immunofluorescence

Control or CD82OE cells were treated as indicated for 48 hours. Cells were blocked in 3% BSA in PBS followed by incubation with primary antibodies (AnnexinV-FITC, 1:200, Biolegend; CD82-Alexa647, 1:200, Biolegend) and DAPI (Invitrogen). Cells were washed and imaged with a Zeiss airyscan (LSM 800) system (Carl Zeiss) using excitation wavelengths of 405, 488 or 633 nm and a 63X/1.2 numerical aperture oil immersion objective.

### Western Blotting

Western blots were performed as previously described (64). Antibodies used for Western blotting were purchased from Cell Signaling Technology as follows: calnexin (C5C9), PKC $\alpha$  (2056), phospho-PKC $\alpha$ / $\beta$  (Thr638/641, 9375), Talin-1 (C45F1), Phospho-Talin-1 (Ser425, D2P2M), p38 (D13E1), phospho-p38 (Thr180/Tyr182, D3F9), or  $\beta$ -Actin (Sigma, AC-74); all antibodies were used at a 1:1000 dilution. Horseradish peroxidase conjugate enzymes were stimulated with SuperSignal West Pico Chemiluminescent Substrate or Femto Maximum Sensitivity Substrate (Life Technologies). Blots were imaged using the ChemiDoc XRS Imager (Bio-Rad) and analyzed using ImageJ (National Institutes of Health) densitometry software.

### Super-resolution imaging

Cells were plated on fibronectin coated eight-well chamber slides and treated with 1.7  $\mu$ M Daunorubicin or vehicle overnight at 37°C. Cells were fixed with 4% PFA, blocked with 3% BSA/PBS and labeled with Alexa Fluor 647 anti-human CD29 antibody (BioLegend, TS2/16, 1:200). Cells were washed and fixed again with 4% PFA. Labeled cells were

imaged in a reducing buffer composed of 50 mM Tris, 10 mM NaCl, 10% w/v glucose, 168.8 u/ml glucose oxidase (Sigma #G2133), 1404.0 U/ml catalase (Sigma #C9332), and 20 mM MEA, pH8.5. Cells were imaged using a custom TIRF microscope system as previously described (20, 64, 76). 40,000 frames were collected per cell, with a brightfield image acquired every 2,000 frames for registration and drift correction. Each frame was  $256 \times 256$  pixels with a pixel size of  $0.107 \mu\text{m}$  and an acquisition time of 10ms per frame.

Instrumentation was controlled by custom-written software in Matlab.

Collected data were analyzed as previously described (77). DBSCAN algorithm was applied to the reconstructed images to assess clustering  $\beta 1$  integrin (parameters:  $\epsilon = 50\text{nm}$  and  $n = 20$ ). Analyses performed using other parameters ( $\epsilon = 100\text{nm}$  and  $n = 30$   $\epsilon = 50\text{nm}$  and  $n = 30$ ) yielded similar clustering and the same trends as our final parameters. Three  $5\mu\text{m} \times 5\mu\text{m}$  ROIs were selected per cell for analysis. Clusters identified by DBSCAN were subjected to the ROUT method of outlier detection (Prism 8, GraphPad) with  $Q = 1\%$ , and identified outliers were removed from further analysis. Cluster radii were calculated using a convex hull around all points identified as a cluster. Equivalent area of a cluster was calculated as  $\text{area} = \pi * R^2$ . Density of clustered points was calculated as the number of localizations in a cluster divided by the cluster area.

## Statistics

Data were analyzed by GraphPad Prism 6 or 8 software. Data are presented as the means  $\pm$  SD/SEM from three independent experiments. At least three biological replicates were performed for each experiment, unless otherwise stated. Two-tailed Student's  $t$  test was used to compare differences between two groups. For comparisons in 3 or more groups One-way ANOVA followed by Tukey's post-hoc test for multiple comparisons. The Kaplan–Meier curves for survival analyses were analyzed using the Log-rank (Mantel-Cox) or Hazard Ratio (Mantel-Haenszel) tests. The Kolmogorov–Smirnov test was used for comparison of cumulative distributions. A  $P$  value  $< 0.05$  was considered statistically significant and significance was labeled as  $*p < 0.05$ ,  $**p < 0.01$ ,  $***p < 0.001$ , and  $****p < 0.0001$ .

## Supplementary Material

Refer to Web version on PubMed Central for supplementary material.

## Acknowledgements

This work was supported by fellowships: F31CA232480 to M.F., F31HL124977 to C.M.T., and T32HL007736 to K.D.M., and an NHLBI investigator grant (ROIHL122483 to J.M.G.), and an American Cancer Society Research Scholar Grant (130675 to J.M.G). This work was partially supported by the UNM Spatiotemporal Modeling Center (P50GM085273) and the UNM Comprehensive Cancer Center Support Grant (P30CA118100) through the following shared resources: Analytical and Translational Genomics, Human Tissue Repository, Fluorescence Microscopy, Flow Cytometry and Biostatistics. We also acknowledge Victoria Balise for critical manuscript review and the experimental assistance of Christian Doyle.

## References:

1. American Cancer Society. Cancer facts & figures. Atlanta, GA: The Society p. volumes.

2. Arber DA, Orazi A, Hasserjian R, Thiele J, Borowitz MJ, Le Beau MM, et al. The 2016 revision to the World Health Organization classification of myeloid neoplasms and acute leukemia. *Blood*. 2016;127(20):2391–405. [PubMed: 27069254]
3. Nasir SS, Giri S, Nunnery S, Martin MG. Outcome of Adolescents and Young Adults Compared With Pediatric Patients With Acute Myeloid and Promyelocytic Leukemia. *Clin Lymphoma Myeloma Leuk*. 2017;17(2):126–32 e1. [PubMed: 27836483]
4. Veuger M, Honders W, Spoelder N, Willemze R, Barge R. Effects of the use of multiple cytotoxic drugs on resistance mechanisms in acute myeloid leukemia. *Leukemia*. 2001;15(3):503–.
5. Zhang J, Gu Y, Chen BA. Mechanisms of drug resistance in acute myeloid leukemia. *Oncotargets Ther*. 2019;12:1937–45.
6. Cloos J, Goemans BF, Hess CJ, van Oostveen JW, Waisfisz Q, Corthals S, et al. Stability and prognostic influence of FLT3 mutations in paired initial and relapsed AML samples. *Leukemia*. 2006;20(7):1217–20. [PubMed: 16642044]
7. El Fakih R, Rasheed W, Hawsawi Y, Alsermani M, Hassanein M. Targeting FLT3 Mutations in Acute Myeloid Leukemia. *Cells*. 2018;7(1).
8. Cook AM, Li L, Ho YW, Lin A, Li L, Stein A, et al. Role of altered growth factor receptor-mediated JAK2 signaling in growth and maintenance of human acute myeloid leukemia stem cells. *Blood*. 2014;123(18):2826–37. [PubMed: 24668492]
9. McCubrey JA, Steelman LS, Abrams SL, Bertrand FE, Ludwig DE, Basecke J, et al. Targeting survival cascades induced by activation of Ras/Raf/MEK/ERK, PI3K/PTEN/Akt/mTOR and Jak/STAT pathways for effective leukemia therapy. *Leukemia*. 2008;22(4):708–22. [PubMed: 18337766]
10. Bosman MC, Schuringa JJ, Vellenga E. Constitutive NF-kappaB activation in AML: Causes and treatment strategies. *Crit Rev Oncol Hematol*. 2016;98:35–44. [PubMed: 26490297]
11. Davoudi Z, Akbarzadeh A, Rahmatiyamchi M, Movassaghpour AA, Alipour M, Nejati-Koshki K, et al. Molecular target therapy of AKT and NF-kB signaling pathways and multidrug resistance by specific cell penetrating inhibitor peptides in HL-60 cells. *Asian Pac J Cancer Prev* 2014;15(10):4353–8. [PubMed: 24935396]
12. Hemler ME. Tetraspanin functions and associated microdomains. *Nat Rev Mol Cell Bio*. 2005;6(10):801–11. [PubMed: 16314869]
13. Hemler ME. Tetraspanin proteins promote multiple cancer stages. *Nat Rev Cancer*. 2014;14(1):49–60. [PubMed: 24505619]
14. Kwon HY, Bajaj J, Ito T, Blevins A, Konuma T, Weeks J, et al. Tetraspanin 3 Is Required for the Development and Propagation of Acute Myelogenous Leukemia. *Cell Stem Cell*. 2015;17(2):152–64. [PubMed: 26212080]
15. Boyer T, Guihard S, Roumier C, Peyrouze P, Gonzales F, Berthon C, et al. Tetraspanin CD81 is an adverse prognostic marker in acute myeloid leukemia. *Oncotarget*. 2016;7(38):62377–85. [PubMed: 27566555]
16. Burchert A, Notter M, Menssen HD, Schwartz S, Knauf W, Neubauer A, et al. CD82 (KAI1), a member of the tetraspan family, is expressed on early haemopoietic progenitor cells and up-regulated in distinct human leukaemias. *Brit J Haematol*. 1999;107(3):494–504. [PubMed: 10583248]
17. Saito-Reis CA, Marjon KD, Pascetti EM, Floren M, Gillette JM. The tetraspanin CD82 regulates bone marrow homing and engraftment of hematopoietic stem and progenitor cells. *Mol Biol Cell*. 2018;29(24):2946–58. [PubMed: 30133344]
18. Nishioka C, Ikezoe T, Yang J, Yokoyama A. Tetraspanin Family Member, CD82, Regulates Expression of EZH2 via Inactivation of p38 MAPK Signaling in Leukemia Cells. *Plos One*. 2015;10(5).
19. Marjon KD, Termini CM, Karlen KL, Saito-Reis C, Soria CE, Lidke KA, et al. Tetraspanin CD82 regulates bone marrow homing of acute myeloid leukemia by modulating the molecular organization of N-cadherin. *Oncogene*. 2016;35(31):4132–40. [PubMed: 26592446]
20. Termini CM, Lidke KA, Gillette JM. Tetraspanin CD82 Regulates the Spatiotemporal Dynamics of PKC alpha in Acute Myeloid Leukemia. *Sci Rep-Uk*. 2016;6.

21. Kurinna S, Konopleva M, Palla SL, Chen W, Kornblau S, Contractor R, et al. Bcl2 phosphorylation and active PKC alpha are associated with poor survival in AML. *Leukemia*. 2006;20(7):1316–9. [PubMed: 16642043]
22. Ruvolo PP, Zhou LR, Watt JC, Ruvolo VR, Burks JK, Jiffar T, et al. Targeting PKC-Mediated Signal Transduction Pathways Using Enzastaurin to Promote Apoptosis in Acute Myeloid Leukemia-Derived Cell Lines and Blast Cells. *J Cell Biochem*. 2011;112(6):1696–707. [PubMed: 21360576]
23. Wakui M, Kuriyama K, Miyazaki Y, Hata T, Taniwaki M, Ohtake S, et al. Diagnosis of acute myeloid leukemia according to the WHO classification in the Japan Adult Leukemia Study Group AML-97 protocol. *Int J Hematol*. 2008;87(2):144–51. [PubMed: 18256787]
24. Walter RB, Othus M, Burnett AK, Lowenberg B, Kantarjian HM, Ossenkoppele GJ, et al. Significance of FAB subclassification of “acute myeloid leukemia, NOS” in the 2008 WHO classification: analysis of 5848 newly diagnosed patients. *Blood*. 2013;121(13):2424–31. [PubMed: 23325837]
25. Byun JM, Kim YJ, Yoon HJ, Kim SY, Kim HJ, Yoon J, et al. Cytogenetic profiles of 2806 patients with acute myeloid leukemia—a retrospective multicenter nationwide study. *Ann Hematol*. 2016;95(8):1223–32. [PubMed: 27230620]
26. Okamoto Y, Kudo K, Tabuchi K, Tomizawa D, Taga T, Goto H, et al. Hematopoietic stem-cell transplantation in children with refractory acute myeloid leukemia. *Bone Marrow Transplant*. 2019;54(9):1489–98. [PubMed: 30718800]
27. Takami M, Katayama K, Noguchi K, Sugimoto Y. Protein kinase C alpha-mediated phosphorylation of PIM-1L promotes the survival and proliferation of acute myeloid leukemia cells. *Biochem Biophys Res Commun*. 2018;503(3):1364–71. [PubMed: 30017192]
28. Efimova T, Deucher A, Kuroki T, Ohba M, Eckert RL. Novel protein kinase C isoforms regulate human keratinocyte differentiation by activating a p38 delta mitogen-activated protein kinase cascade that targets CCAAT/enhancer-binding protein alpha. *J Biol Chem*. 2002;277(35):31753–60. [PubMed: 12080077]
29. Hocevar BA, Morrow DM, Tykocinski ML, Fields AP. Protein kinase C isotypes in human erythroleukemia cell proliferation and differentiation. *J Cell Sci*. 1992;101 ( Pt 3):671–9. [PubMed: 1522149]
30. Myklebust JH, Smeland EB, Josefsen D, Sioud M. Protein kinase C-alpha isoform is involved in erythropoietin-induced erythroid differentiation of CD34(+) progenitor cells from human bone marrow. *Blood*. 2000;95(2):510–8. [PubMed: 10627456]
31. Jin JK, Tien PC, Cheng CJ, Song JH, Huang C, Lin SH, et al. Talin1 phosphorylation activates beta1 integrins: a novel mechanism to promote prostate cancer bone metastasis. *Oncogene*. 2015;34(14):1811–21. [PubMed: 24793790]
32. Ramirez P, Rettig MP, Uy GL, Deych E, Holt MS, Ritchey JK, et al. BIO5192, a small molecule inhibitor of VLA-4, mobilizes hematopoietic stem and progenitor cells. *Blood*. 2009;114(7):1340–3. [PubMed: 19571319]
33. van Kooyk Y, Figdor CG. Avidity regulation of integrins: the driving force in leukocyte adhesion. *Curr Opin Cell Biol*. 2000;12(5):542–7. [PubMed: 10978887]
34. Kolanus W, Seed B. Integrins and inside-out signal transduction: converging signals from PKC and PIP3. *Curr Opin Cell Biol*. 1997;9(5):725–31. [PubMed: 9330877]
35. Martin Ester H-PK, Jorg Sander, Xiaowei Xu. A density-based algorithm for discovering clusters in large spatial databases with noise. In *Proceedings of the 2nd International Conference on Knowledge Discovery and Data Mining 1996*; AAAI Press:226–31.
36. Thornton TM, Rincon M. Non-classical p38 map kinase functions: cell cycle checkpoints and survival. *Int J Biol Sci*. 2009;5(1):44–51. [PubMed: 19159010]
37. Wood CD, Thornton TM, Sabio G, Davis RA, Rincon M. Nuclear localization of p38 MAPK in response to DNA damage. *Int J Biol Sci*. 2009;5(5):428–37. [PubMed: 19564926]
38. Gupta J, Igea A, Papaioannou M, Lopez-Casas PP, Llonch E, Hidalgo M, et al. Pharmacological inhibition of p38 MAPK reduces tumor growth in patient-derived xenografts from colon tumors. *Oncotarget* 2015;6(11):8539–51. [PubMed: 25890501]

39. Naci D, Aoudjit F. Alpha2beta1 integrin promotes T cell survival and migration through the concomitant activation of ERK/Mcl-1 and p38 MAPK pathways. *Cell Signal*. 2014;26(9):2008–15. [PubMed: 24880062]
40. Scott MJ, Billiar TR. Beta2-integrin-induced p38 MAPK activation is a key mediator in the CD14/TLR4/MD2-dependent uptake of lipopolysaccharide by hepatocytes. *J Biol Chem*. 2008;283(43):29433–46. [PubMed: 18701460]
41. Hwang S, Takimoto T, Hemler ME. Integrin-independent support of cancer drug resistance by tetraspanin CD151. *Cell Mol Life Sci*. 2019;76(8):1595–604. [PubMed: 30778617]
42. Ye M, Wei T, Wang Q, Sun Y, Tang R, Guo L, et al. TSPAN12 promotes chemoresistance and proliferation of SCLC under the regulation of miR-495. *Biochem Biophys Res Commun*. 2017;486(2):349–56. [PubMed: 28302484]
43. Kohmo S, Kijima T, Otani Y, Mori M, Minami T, Takahashi R, et al. Cell surface tetraspanin CD9 mediates chemoresistance in small cell lung cancer. *Cancer Res*. 2010;70(20):8025–35. [PubMed: 20940407]
44. Ullah M, Akbar A, Ng NN, Concepcion W, Thakor AS. Mesenchymal stem cells confer chemoresistance in breast cancer via a CD9 dependent mechanism. *Oncotarget* 2019;10(37):3435–50. [PubMed: 31191817]
45. Nishioka C, Ikezoe T, Yang J, Nobumoto A, Kataoka S, Tsuda M, et al. CD82 regulates STAT5/IL-10 and supports survival of acute myelogenous leukemia cells. *Int J Cancer*. 2014;134(1):55–64. [PubMed: 23797738]
46. Ji H, Chen L, Xing Y, Li S, Dai J, Zhao P, et al. CD82 supports survival of childhood acute myeloid leukemia cells via activation of Wnt/beta-catenin signaling pathway. *Pediatr Res*. 2019;85(7):1024–31. [PubMed: 30862962]
47. Nishioka C, Ikezoe T, Takeuchi A, Nobumoto A, Tsuda M, Yokoyama A. The novel function of CD82 and its impact on BCL2L12 via AKT/STAT5 signal pathway in acute myelogenous leukemia cells. *Leukemia*. 2015;29(12):2296–306. [PubMed: 26260387]
48. Bonardi F, Fusetti F, Deelen P, van Gosliga D, Vellenga E, Schuringa JJ. A proteomics and transcriptomics approach to identify leukemic stem cell (LSC) markers. *Mol Cell Proteomics*. 2013;12(3):626–37. [PubMed: 23233446]
49. Tonoli H, Barrett JC. CD82 metastasis suppressor gene: a potential target for new therapeutics? *Trends Mol Med*. 2005;11(12):563–70. [PubMed: 16271511]
50. Miranti CK. Controlling cell surface dynamics and signaling: how CD82/KAI1 suppresses metastasis. *Cell Signal*. 2009;21(2):196–211. [PubMed: 18822372]
51. Tsai YC, Weissman AM. Dissecting the diverse functions of the metastasis suppressor CD82/KAI1. *FEBS Lett*. 2011;585(20):3166–73. [PubMed: 21875585]
52. Nishioka C, Ikezoe T, Furihata M, Yang J, Serada S, Naka T, et al. CD34+/CD38 acute myelogenous leukemia cells aberrantly express CD82 which regulates adhesion and survival of leukemia stem cells. *Int J Cancer*. 2013;132(9):2006–19. [PubMed: 23055153]
53. Ruvolo PP, Zhou L, Watt JC, Ruvolo VR, Burks JK, Jiffar T, et al. Targeting PKC-mediated signal transduction pathways using enzastaurin to promote apoptosis in acute myeloid leukemia-derived cell lines and blast cells. *J Cell Biochem*. 2011;112(6):1696–707. [PubMed: 21360576]
54. Brockstein B, Samuels B, Humerickhouse R, Arietta R, Fishkin P, Wade J, et al. Phase II studies of bryostatin-1 in patients with advanced sarcoma and advanced head and neck cancer. *Invest New Drugs*. 2001;19(3):249–54. [PubMed: 11561683]
55. Varterasian ML, Mohammad RM, Shurafa MS, Hulburd K, Pemberton PA, Rodriguez DH, et al. Phase II trial of bryostatin 1 in patients with relapsed low-grade non-Hodgkin's lymphoma and chronic lymphocytic leukemia. *Clin Cancer Res*. 2000;6(3):825–8. [PubMed: 10741703]
56. Crump M, Leppa S, Fayad L, Lee JJ, Di Rocco A, Ogura M, et al. Randomized, Double-Blind, Phase III Trial of Enzastaurin Versus Placebo in Patients Achieving Remission After First-Line Therapy for High-Risk Diffuse Large B-Cell Lymphoma. *J Clin Oncol* 2016;34(21):2484–92. [PubMed: 27217449]
57. Aoudjit F, Vuori K. Integrin signaling in cancer cell survival and chemoresistance. *Chemother Res Pract*. 2012;2012:283181. [PubMed: 22567280]

58. Naci D, El Azreq MA, Chetoui N, Lauden L, Sigaux F, Charron D, et al. alpha2beta1 integrin promotes chemoresistance against doxorubicin in cancer cells through extracellular signal-regulated kinase (ERK). *J Biol Chem.* 2012;287(21):17065–76. [PubMed: 22457358]
59. Nair MG, Desai K, Prabhu JS, Hari PS, Remacle J, Sridhar TS. beta3 integrin promotes chemoresistance to epirubicin in MDA-MB-231 through repression of the pro-apoptotic protein, BAD. *Exp Cell Res.* 2016;346(1):137–45. [PubMed: 27235542]
60. Sansing HA, Sarkeshik A, Yates JR, Patel V, Gutkind JS, Yamada KM, et al. Integrin alphabeta1, alphavbeta, alpha6beta effectors p130Cas, Src and talin regulate carcinoma invasion and chemoresistance. *Biochem Biophys Res Commun.* 2011;406(2):171–6. [PubMed: 21291860]
61. Seguin L, Desgrosellier JS, Weis SM, Cheresh DA. Integrins and cancer: regulators of cancer stemness, metastasis, and drug resistance. *Trends Cell Biol.* 2015;25(4):234–40. [PubMed: 25572304]
62. Berrazouane S, Boisvert M, Salti S, Mourad W, Al-Daccak R, Barabe F, et al. Beta1 integrin blockade overcomes doxorubicin resistance in human T-cell acute lymphoblastic leukemia. *Cell Death Dis.* 2019;10(5):357. [PubMed: 31043590]
63. Zhang XA, Bontrager AL, Hemler ME. Transmembrane-4 superfamily proteins associate with activated protein kinase C (PKC) and link PKC to specific beta(1) integrins. *J Biol Chem.* 2001;276(27):25005–13. [PubMed: 11325968]
64. Termini CM, Cotter ML, Marjon KD, Buranda T, Lidke K, Gillette JM. Regulation of VLA-4 mediated hematopoietic stem/progenitor cell adhesion by CD82. *Mol Biol Cell.* 2012;23.
65. Bachegowda L, Morrone K, Winski SL, Mantzaris I, Bartenstein M, Ramachandra N, et al. Pexmetinib: A Novel Dual Inhibitor of Tie2 and p38 MAPK with Efficacy in Preclinical Models of Myelodysplastic Syndromes and Acute Myeloid Leukemia. *Cancer Res.* 2016;76(16):4841–9. [PubMed: 27287719]
66. Garcia-Manero G, Khoury HJ, Jabbour E, Lancet J, Winski SL, Cable L, et al. A phase I study of oral ARRY-614, a p38 MAPK/Tie2 dual inhibitor, in patients with low or intermediate-1 risk myelodysplastic syndromes. *Clin Cancer Res.* 2015;21(5):985–94. [PubMed: 25480830]
67. Beckwith KA, Byrd JC, Muthusamy N. Tetraspanins as therapeutic targets in hematological malignancy: a concise review. *Front Physiol* 2015;6:91. [PubMed: 25852576]
68. Brown RB, Madrid NJ, Suzuki H, Ness SA. Optimized approach for Ion Proton RNA sequencing reveals details of RNA splicing and editing features of the transcriptome. *Plos One.* 2017;12(5):e0176675. [PubMed: 28459821]
69. Brayer KJ, Frerich CA, Kang H, Ness SA. Recurrent Fusions in MYB and MYBL1 Define a Common, Transcription Factor-Driven Oncogenic Pathway in Salivary Gland Adenoid Cystic Carcinoma. *Cancer Discov.* 2016;6(2):176–87. [PubMed: 26631070]
70. Frerich CA, Brayer KJ, Painter BM, Kang H, Mitani Y, El-Naggar AK, et al. Transcriptomes define distinct subgroups of salivary gland adenoid cystic carcinoma with different driver mutations and outcomes. *Oncotarget.* 2018;9(7):7341–58. [PubMed: 29484115]
71. Anders S, Pyl PT, Huber W. HTSeq--a Python framework to work with high-throughput sequencing data. *Bioinformatics.* 2015;31(2):166–9. [PubMed: 25260700]
72. Robinson MD, McCarthy DJ, Smyth GK. edgeR: a Bioconductor package for differential expression analysis of digital gene expression data. *Bioinformatics.* 2010;26(1):139–40. [PubMed: 19910308]
73. Varet H, Brillet-Gueguen L, Coppee JY, Dillies MA. SARTools: A DESeq2- and EdgeR-Based R Pipeline for Comprehensive Differential Analysis of RNA-Seq Data. *Plos One.* 2016;11(6):e0157022. [PubMed: 27280887]
74. Saldanha AJ. Java Treeview--extensible visualization of microarray data. *Bioinformatics.* 2004;20(17):3246–8. [PubMed: 15180930]
75. Zhou Y, Zhou B, Pache L, Chang M, Khodabakhshi AH, Tanaseichuk O, et al. Metascape provides a biologist-oriented resource for the analysis of systems-level datasets. *Nat Commun.* 2019;10(1):1523. [PubMed: 30944313]
76. Valley CC, Liu S, Lidke DS, Lidke KA. Sequential superresolution imaging of multiple targets using a single fluorophore. *Plos One.* 2015;10(4):e0123941. [PubMed: 25860558]

77. Huang F, Schwartz SL, Byars JM, Lidke KA. Simultaneous multiple-emitter fitting for single molecule super-resolution imaging. *Biomed Opt Express*. 2011;2(5):1377–93. [PubMed: 21559149]

Author Manuscript

Author Manuscript

Author Manuscript

Author Manuscript



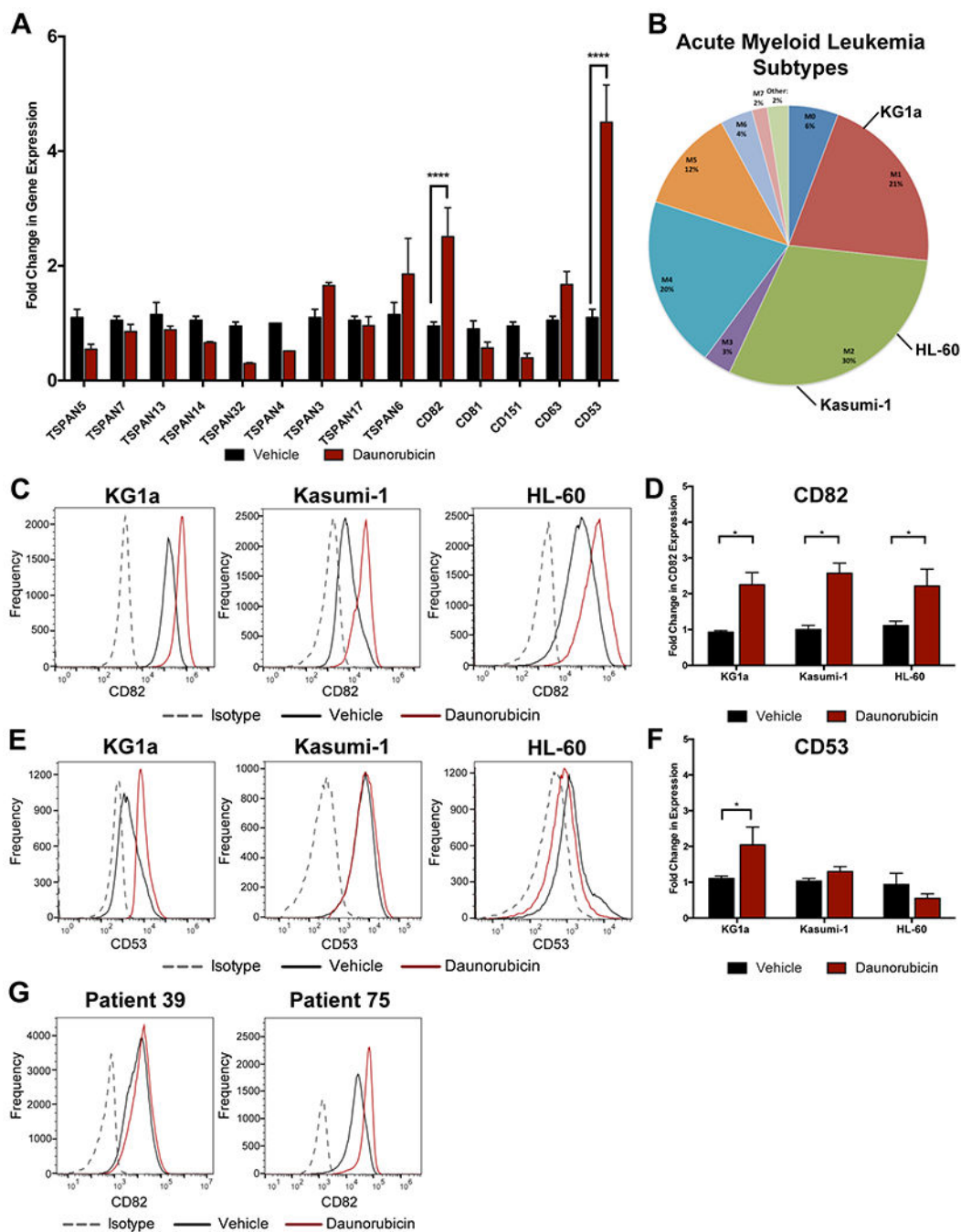


**Figure 1: Chemotherapy increases the expression of tetraspanin CD82 in AML.**

(A) Tetraspanin gene expression profile based on RNA-seq analysis of vehicle or daunorubicin (1.7 $\mu$ M) treated KG1a control cells following 24 hr. (B) Analysis of AML prevalence by French-American-British (FAB) classification subtypes. Flow cytometry histograms measuring surface expression of (C) CD82 or (E) CD53 following vehicle or daunorubicin (1.7 $\mu$ M) treatment for 24 hr. (D) Fold Change in protein expression of (D) CD82 or (F) CD53 in different AML cell lines treated with vehicle or daunorubicin (1.7 $\mu$ M) for 24 hr measured by flow cytometry (n=3). (G) Flow cytometry analysis of CD82 surface

expression in AML patient samples following treatment with vehicle or daunorubicin (1.7 $\mu$ M) for 24 hr. Means  $\pm$  SD ( $n = 2$  in A, 3 in C-F) \* $p < 0.05$ , and \*\*\*\* $p < 0.0001$ .

Author Manuscript

Author Manuscript

Author Manuscript

Author Manuscript

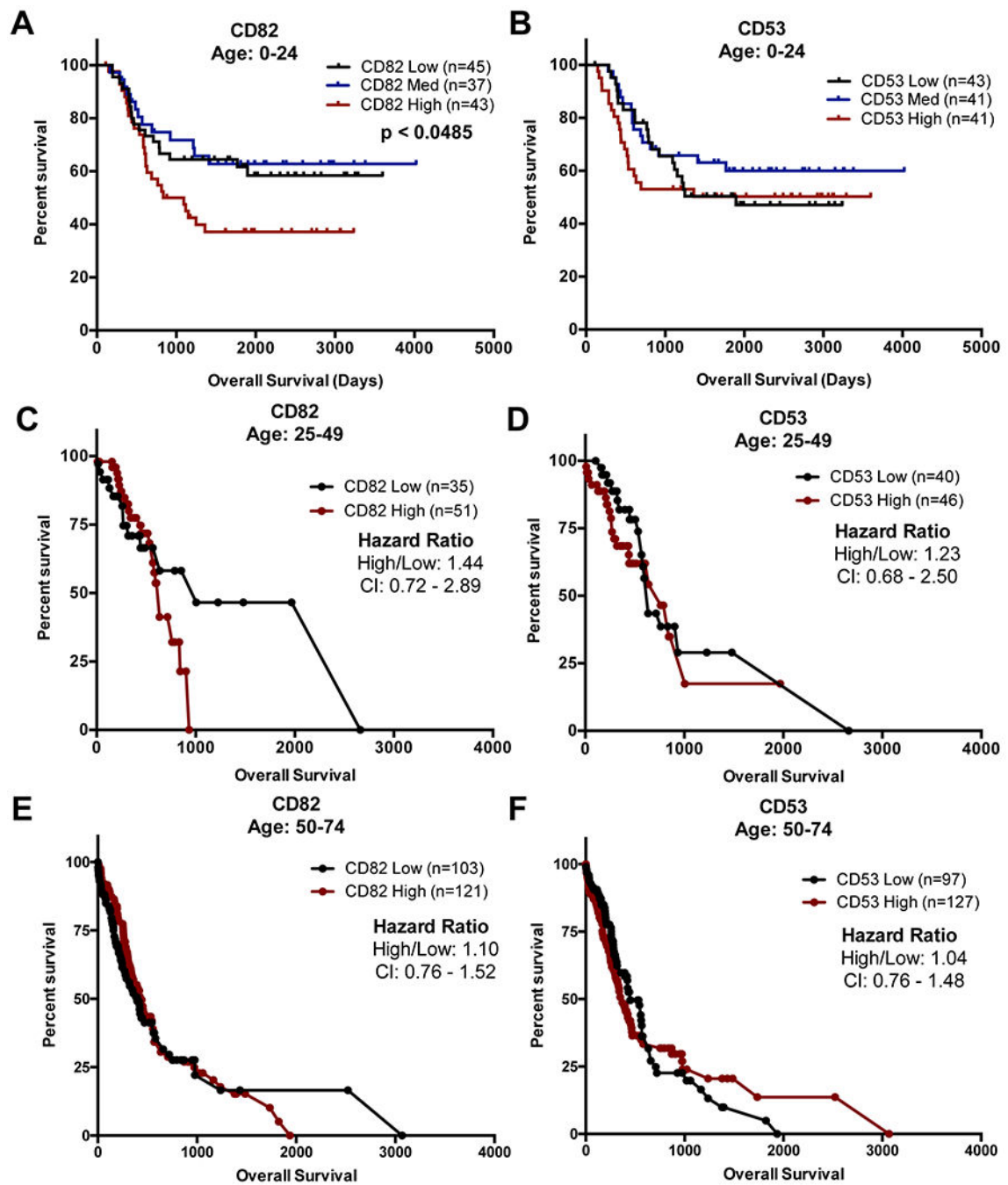


**Figure 2: Increased CD82 expression in AML patient samples correlates with reduced overall survival.**

Kaplan-Myer survival curve analysis for overall survival of 125 pediatric AML patients (Ages:0-24) from the TARGET database by (A) CD82 and (B) CD53 expression. Kaplan-Myer survival curve analysis for 310 adult AML patients (Ages:25-74) included in the BEAT AML trial based on (C, E) CD82 or (D, F) CD53 expression.

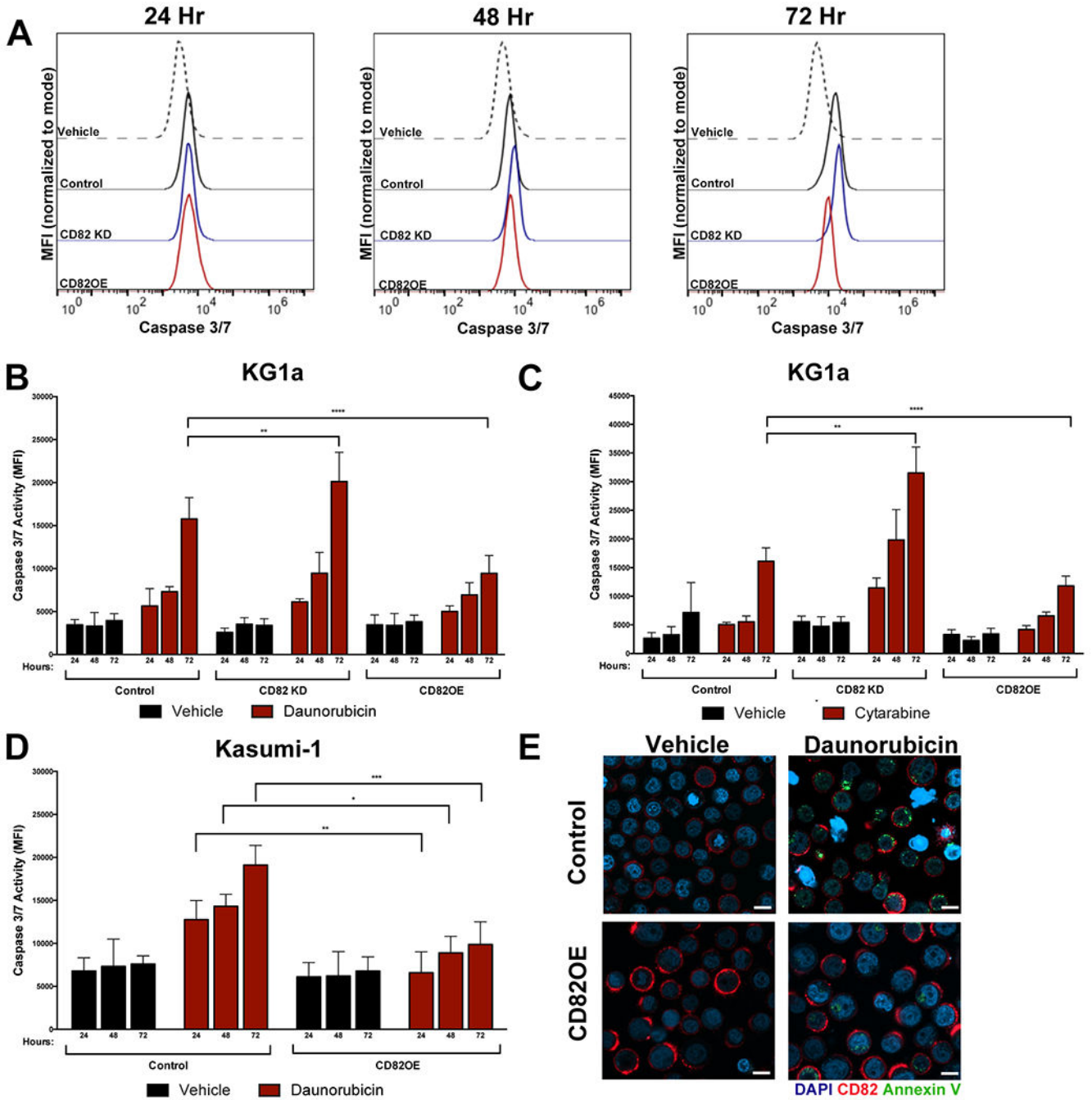


**Figure 3: CD82 overexpression promotes AML chemoresistance.**

Caspase activity was measured in KG1a cell lines differentially expressing CD82, which were treated with vehicle (A, B), 1.7µM daunorubicin or (C) 0.5µM cytarabine over 72 hours. (C) Caspase activity was measured in Kasumi-1 cells transfected with mCherry vector control or mCherry-CD82 and treated with vehicle or 1.7µM daunorubicin over 72 hours. (D) Control and CD82OE KG1a cells were treated with vehicle or 1.7µM daunorubicin for 24 hr and then fixed and stained for apoptosis marker, Annexin V (green), CD82 (red) and DAPI (blue) and imaged by confocal microscopy Scale bars: 10 µm. Means

$\pm$  SD ( $n = 3$  in A - E). 2-Way ANOVA statistical significance in B - D is in comparison to the matching time-point of vehicle treated control cells. \* $p < 0.05$ , \*\* $p < 0.01$  and \*\*\*\* $p < 0.0001$ .

Author Manuscript

Author Manuscript

Author Manuscript

Author Manuscript

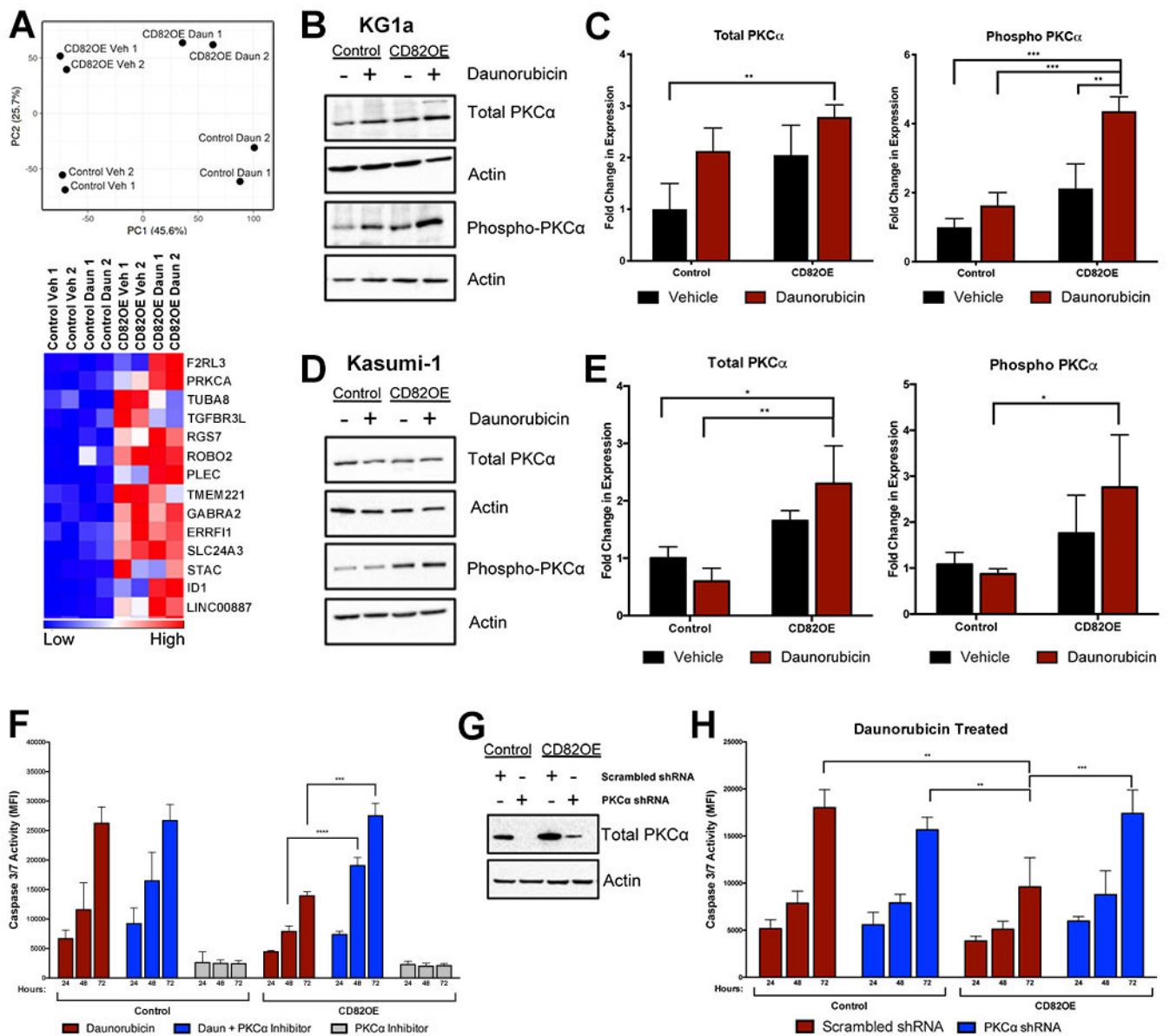


**Figure 4: PKC $\alpha$  is required for CD82-mediated chemoresistance**

(A) Principal component analysis and condensed heatmap for control and CD82OE cells treated with vehicle or Daunorubicin. Total and phospho-PKC $\alpha$  levels were analyzed by Western blot in control and CD82OE cells: KG1a (B, C) and Kasumi-1 (D, E). (F) Caspase activity measured in KG1a cells with PKC $\alpha$  inhibitor, Go 6976 (2.5 nM), alone or in combination with 1.7 $\mu$ M daunorubicin. (G) Western blot analysis for PKC $\alpha$  24hr after shRNA transfection of KG1a cells. (H) Caspase activity measured in PKC $\alpha$  shRNA or scrambled shRNA treated control or CD82OE KG1a cells, which were treated with 1.7 $\mu$ M daunorubicin. Means  $\pm$  SD ( $n = 2$  in A, 3 in B - H) \* $p < 0.05$ , \*\* $p < 0.01$  and \*\*\* $p < 0.001$ .

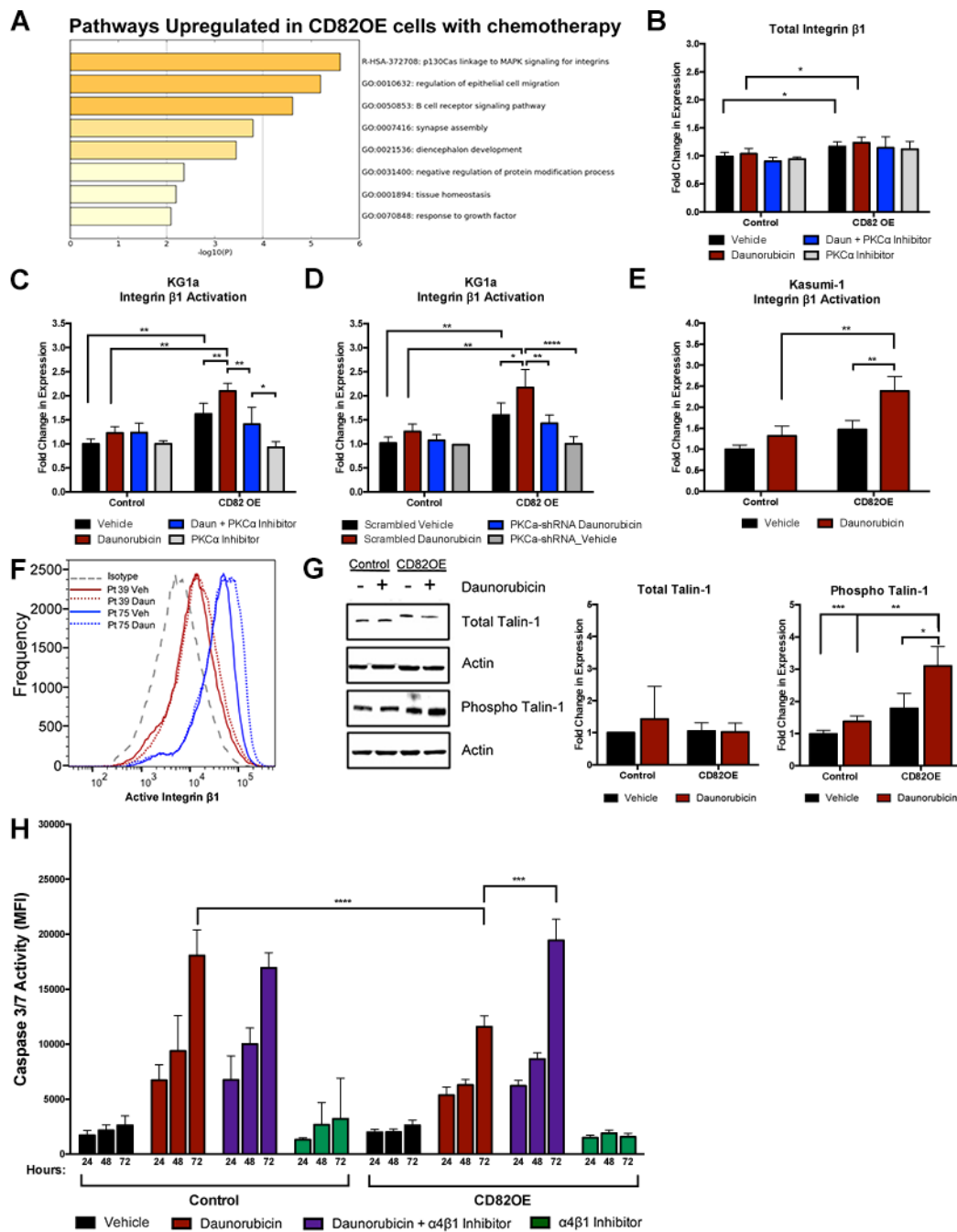


**Figure 5: Chemotherapy activates  $\beta$ 1 integrin downstream of PKC $\alpha$ .**

(A) Pathway analysis for genes upregulated in CD82OE cells upon treatment with daunorubicin. (B) Total and (C) active  $\beta$ 1 integrin levels were analyzed by flow cytometry in control and CD82OE KG1a cells 24 hours after treatment with vehicle, daunorubicin (1.7 $\mu$ M), PKC $\alpha$  inhibitor, Go 6976 (2.5 nM), or Go 6976 (2.5 nM) and daunorubicin (1.7 $\mu$ M). (D) Active  $\beta$ 1 integrin levels were measured by flow cytometry following PKC $\alpha$  shRNA or scrambled shRNA treatment of control and CD82OE KG1a cells, that were treated for 24 hr with vehicle or daunorubicin (1.7 $\mu$ M).  $\beta$ 1 integrin activation was quantified

by flow cytometry in **(E)** control or CD82OE Kasumi-1 cells and **(F)** primary AML patient samples following vehicle or daunorubicin (1.7 $\mu$ M) treatment for 24 hr. **(G)** Western blot analysis of total and phospho-Talin-1 levels analyzed in control and CD82OE KG1a cells 24 hours after treatment with vehicle or daunorubicin (1.7 $\mu$ M). **(H)** Caspase activity was measured in control and CD82OE KG1a cells following treatment with vehicle, daunorubicin (1.7 $\mu$ M),  $\alpha$ 4 $\beta$ 1 integrin inhibitor, Bio 5192 (20 nM) or Bio 5192 (20 nM) in combination with daunorubicin (1.7 $\mu$ M) over 72 hours. Means  $\pm$  SD ( $n = 2$  in A, 3 in B – E, 2 in F, 3 in G and H) \* $p < 0.05$ , \*\* $p < 0.01$ , \*\*\* $p < 0.001$  and \*\*\*\* $p < 0.0001$ .



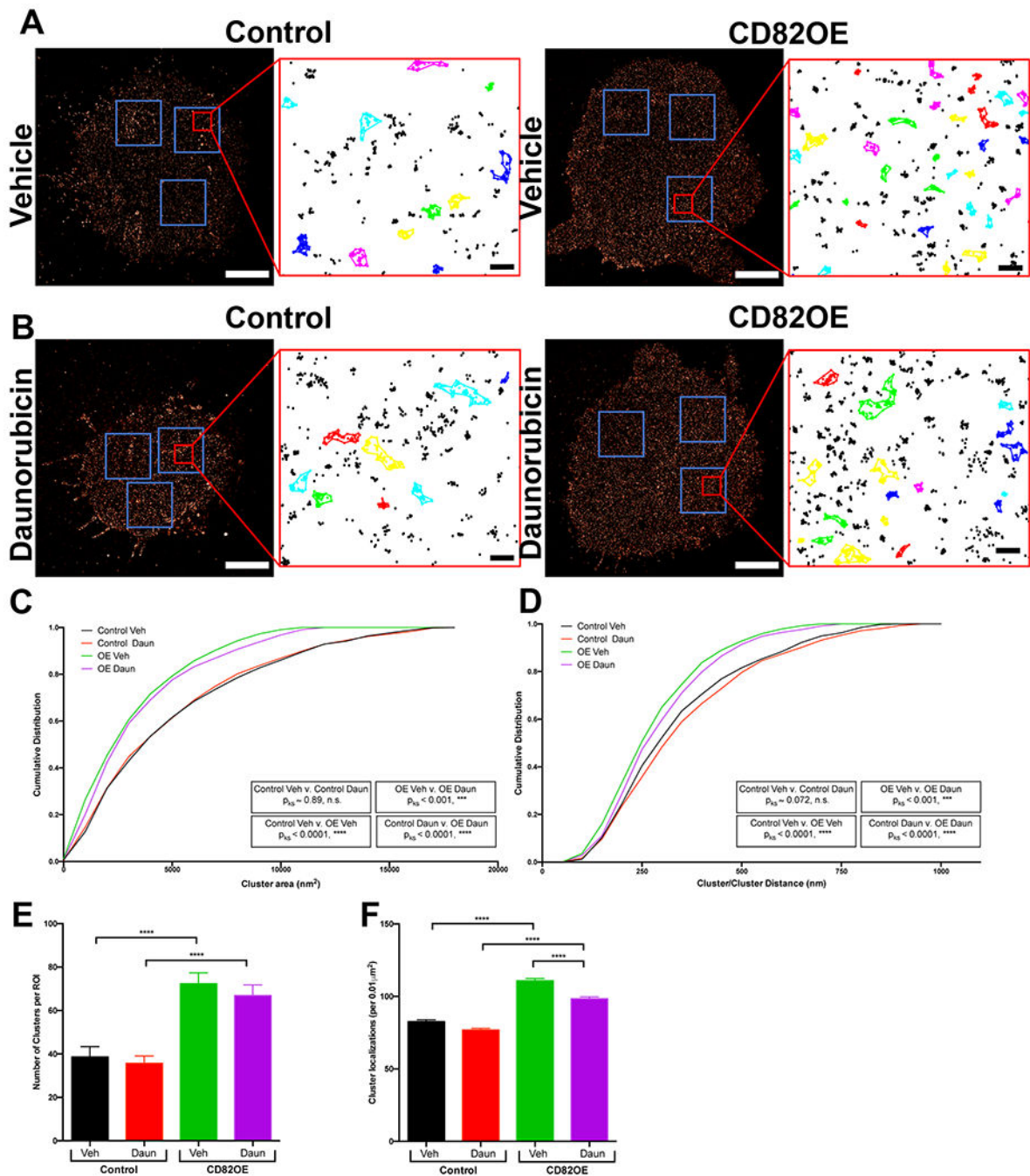


**Figure 6: CD82 expression alters  $\beta 1$  integrin membrane clustering.**

Representative dSTORM images of control and CD82OE KG1a cells labeled for  $\beta 1$  integrin after treatment with (A) vehicle or (B) 1.7  $\mu\text{M}$  daunorubicin. Blue boxes represent  $5 \times 5 \mu\text{m}$  ROIs used for clustering analysis; scale bar: 5  $\mu\text{m}$ . Enlarged regions show  $\beta 1$  integrin clustering determined by DBSCAN analysis; parameters used were  $\epsilon = 50\text{nm}$  and  $n = 20$  points; scale bar = 200nm. Cumulative distribution plots of (C) cluster area and (D) cluster-to-cluster distance were derived from DBSCAN clustering data; statistical significance determined using the Kolmogorov-Smirnov test. (E) Average number of clusters per ROI

and **(F)** average number of cluster localizations per  $0.01\mu\text{m}^2$  were determined using DBSCAN. For all analyses,  $n = 9$  cells per condition. Error bars, SEM; \*\*\* $p < 0.001$  and \*\*\*\* $p < 0.0001$ .

Author Manuscript

Author Manuscript

Author Manuscript

Author Manuscript

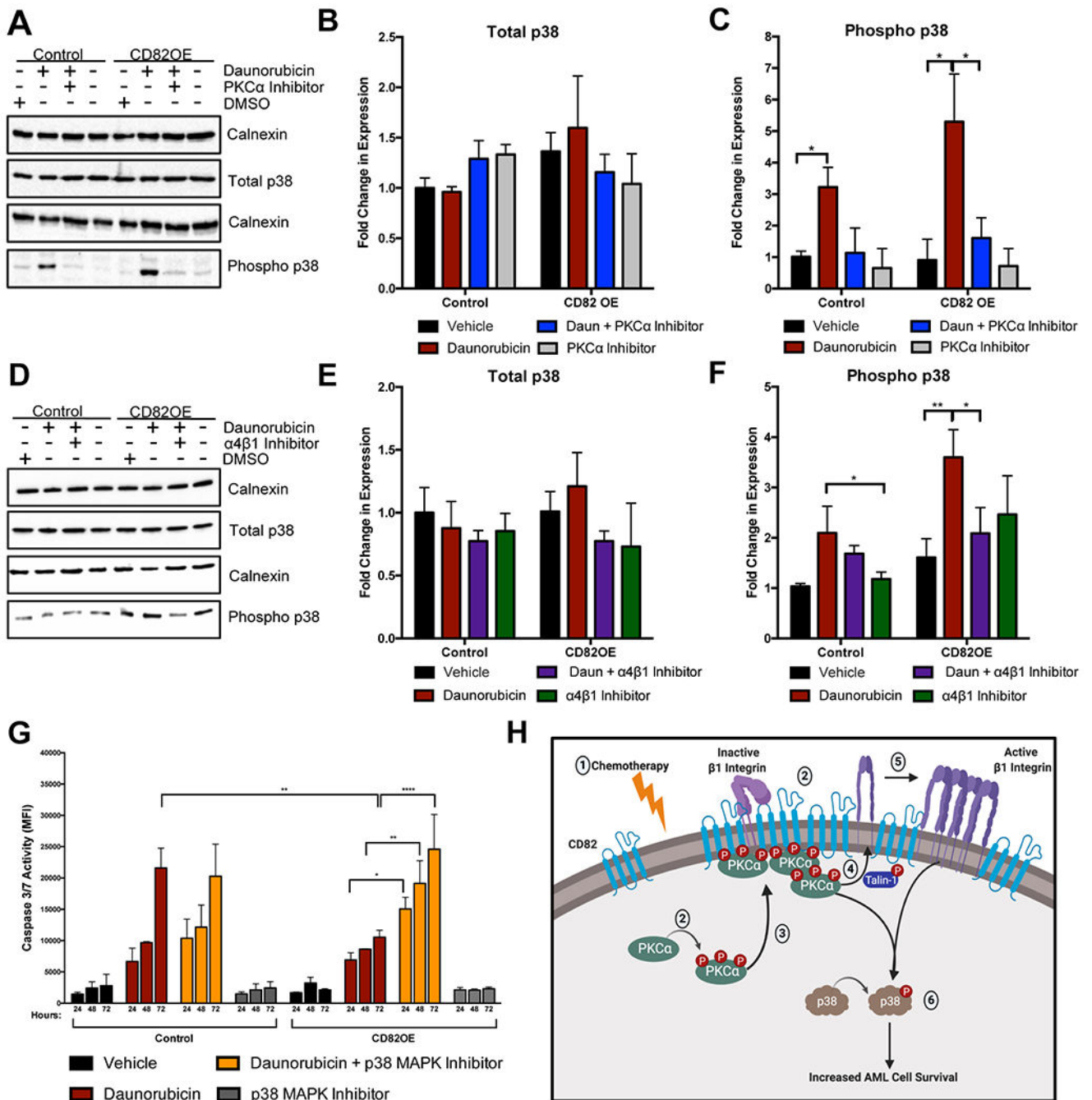


**Figure 7: Chemotherapy activates p38 MAPK downstream of PKC $\alpha$  and  $\beta$ 1 integrin signaling.**

(A) Western blot analysis of total and phospho-p38 levels in control and CD82OE KG1a cells 24 hours after treatment with vehicle, daunorubicin (1.7 $\mu$ M), Go 6976 (2.5 nM), or Go 6976 (2.5 nM) in combination with daunorubicin (1.7 $\mu$ M). Densitometry analysis of total (B) and phospho-p38 (C) Western blots from (A). (D) Western blot analysis of total and phospho-p38 levels in control and CD82OE KG1a cells 24 hours after treatment with vehicle, daunorubicin (1.7 $\mu$ M), Bio 5192 (20 nM), or Bio5192 (20 nM) in combination with daunorubicin (1.7 $\mu$ M). Densitometry analysis of total (E) and phospho-p38 (F) Western

blots from (D). (G) Caspase activity was measured in control and CD82OE KG1a cells following treatment with vehicle, daunorubicin (1.7 $\mu$ M), p38 MAPK inhibitor, BMS 582949 (25 nM) or BMS 582949 (25 nM) in combination with daunorubicin (1.7 $\mu$ M) over 72 hours. (H) Schematic model of CD82 mediated chemoresistance (created using BioRender). Chemotherapy treatment (1) stimulates increased CD82 surface expression and PKC $\alpha$  activation (2), which promotes PKC $\alpha$  localization to the plasma membrane (3). Active PKC $\alpha$  stimulates the activation of  $\beta$ 1 integrin via talin-1 mediated inside out signaling (4) and increased CD82 expression promotes  $\beta$ 1 integrin clustering (5). p38 MAPK is activated downstream of PKC $\alpha$  and  $\beta$ 1 integrin activation promoting increased AML cell survival (6). ( $n = 3$  in A – F) \* $p < 0.05$  and \*\* $p < 0.01$  and \*\*\*\* $p < 0.0001$ .